

Metal-Free Activation of Dioxygen by Graphene/g-C₃N₄ Nanocomposites: Functional Dyads for Selective Oxidation of Saturated Hydrocarbons

Xin-Hao Li,^{*,†} Jie-Sheng Chen,[‡] Xinchen Wang,[†] Jianhua Sun,[†] and Markus Antonietti[†]

[†]Department of Colloid Chemistry, Max-Planck Institute of Colloids and Interfaces, Research Campus Golm, 14424 Postdam, Germany

[‡]School of Chemistry and Chemical Engineering, Shanghai Jiao Tong University, Shanghai 200240, P.R. China

S Supporting Information

ABSTRACT: Graphene sheet/polymeric carbon nitride nanocomposite (GSCN) functions as a metal-free catalyst to activate O₂ for the selective oxidation of secondary C–H bonds of cyclohexane. By fine-tuning the weight ratio of graphene and carbon nitride components, GSCN offers good conversion and high selectivity to corresponding ketones. Besides its high stability, this catalyst also exhibits high chemoselectivity for secondary C–H bonds of various saturated alkanes and, therefore, should be useful in overcoming challenges confronted by metal-mediated catalysis.

Catalytic oxidation of saturated C–H bonds of less expensive alkanes to high-value-added chemicals remains a significant task in many important current industrial and fine-chemical processes.¹ Among various catalytic systems, selective oxidation using environmentally benign molecular oxygen is one of the most problematic processes to control, because the abundance and inertness of the C–H bonds in organic structures present difficulties for selectivity, and the molecular oxygen often results in overoxidation. In nature, enzymes use binding and proximity effects to achieve astounding rate and selectivity enhancements for specific reactions and substrates under mild conditions.² An important new area of bioinorganic chemistry is devoted to the simulation of the enzymatic functions with transition-metal complexes as homogeneous catalysts, which could lead to unprecedented activities and selectivities.³ Typically, the transition-metal centers in the enzymes play a key role in activating the molecular oxygen, where sacrificial catalysts are usually involved;^{1–3} therefore, they are blue-prints for the design of biomimetic oxidation catalysts.

Thus far, efficient O₂-based catalytic oxidations of saturated alkanes in the chemical industry are only compatible with the production of terephthalic acid and cyclohexanone using metal-complex catalysts.¹ The corresponding processes mostly apply homogeneous metal catalysts with the assistance of a large amount of acid to offer only moderate selectivities.^{1a–d} Recyclable catalysts that are stable but active are still highly desirable to further decrease the economic and environmental costs of those processes. The ideal sustainable catalytic oxidation process would use molecular oxygen as the only oxygen source, a recyclable and inexpensive catalyst in nontoxic solvents with good conversion and selectivity, and an inexpensive energy source.^{1a,3}

Recently, we introduced g-C₃N₄ as a heterogeneous, metal-free organocatalyst for Friedel–Crafts reactions, CO₂ fixation, and artificial photosynthesis.⁴ As the most stable phase of C₃N₄ at ambient conditions, a polymeric, slightly distorted g-C₃N₄ can be prepared via thermal polycondensation of common monomers for the price of a typical mass polymer. Thus, this abundant, stable, and metal-free polymeric solid could fulfill the requirements for use as an industrial catalyst. Both the composition and the properties of g-C₃N₄ can be further engineered by introducing selected heteroatoms,⁵ which could slightly modify the molecular orbital shape and position, such as the HOMO relevant for oxidation, and therefore the oxidation strength and the selectivity. Another possibility to do so is the one applied here, which is by environment and by charge-transfer complexation to form a nanocomposite with an electron-rich system,⁶ thus moving electron density within the catalyst.

Herein, we report the activation of molecular oxygen for the selective oxidation of sp³ C–H bonds catalyzed by a graphene sheet (GS)/polymeric carbon nitride (g-C₃N₄) nanocomposite in a heterogeneous situation. A synergistic effect of GS and g-C₃N₄ on promoting the catalytic activation of molecular oxygen was observed, which is not found for either bare g-C₃N₄ or GS alone. This system also showed high selectivity toward ketones and high compatibility with various substrates. Our study provides an ideal example of heterogeneous and sustainable catalysts that can achieve highly selective, O₂-based oxidation of nonactivated secondary C–H bonds without the employment of any metal components and co-reducing agents.⁷ Recently, we reported the oxidation of activated methyl groups by B-doped g-C₃N₄, but the catalyst gave no conversion of nonactivated C–H bonds.^{5c}

Monolayer GSs were selected as the electron-donating modifier for g-C₃N₄ due to their layered structure similar to g-C₃N₄ and their suitable electronic, mechanical, and chemical properties.⁸ A recently described photochemical reduction technique is applied to generate stable aqueous colloids of clean GSs from graphene oxide.⁹ The GSs exhibit monolayer structure (Figure 1a) with a thickness around 0.9 nm (also see Supporting Information, Figure S1). The homogeneous distribution of GSs in both the precursor (cyanamide) and the bulk phase of g-C₃N₄ is key for preparing high-quality nanocomposites. Figure 1b shows the zeta potentials of the GS solution in the presence of

Received: February 1, 2011

Published: May 11, 2011

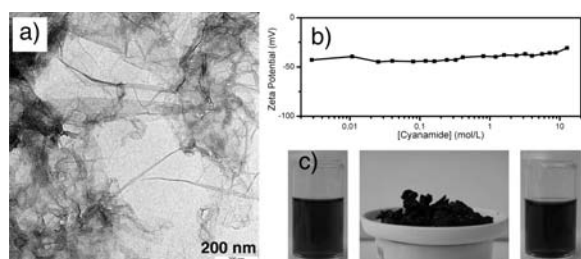


Figure 1. (a) TEM image of GS. (b) Zeta potential of GS in a cyanamide solution with different concentrations. (c) Photos of mixtures of GS and cyanamide in forms of colloidal solution (left), dry powder (middle), and redispersed solution (right).

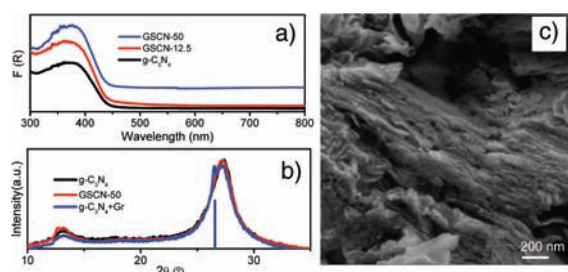


Figure 2. (a) UV-vis absorbance spectra of $g\text{-C}_3\text{N}_4$ and GSCN- x . (b) XRD patterns of $g\text{-C}_3\text{N}_4$, GSCN-50, and a ground mixture of $g\text{-C}_3\text{N}_4$ (3 g) and highly reduced r-GO (Gr, 50 mg, prepared by heating r-GO powder at 873 K for 8 h in N_2). (c) SEM image of GSCN-20.

different amounts of cyanamide, unambiguously revealing that the introduction of cyanamide never disturbs the colloidal stability of GS colloids. After removing the water from the dark brown solution (Figure 1c, left), we obtained gray or black powder (Figure 1c, middle), which could be redispersed into water to form a homogeneous dispersion without visible aggregation (Figure 1c, right). This phenomenon gives direct evidence of the homogeneous distribution of r-GO in cyanamide solid. Further heat treatment at 873 K could simultaneously trigger the thermal condensation of cyanamide to polymeric $g\text{-C}_3\text{N}_4$ and further the deep reduction of GS. For simplicity, the graphene/ $g\text{-C}_3\text{N}_4$ composites are denoted as GSCN- x , where x (2.5, 12.5, 25, or 50 mg) refers to the weighed-in amount of GS per batch.

The presence of GS in GSCN can be directly observed from the color change from yellow ($g\text{-C}_3\text{N}_4$) to dark green. UV-vis spectra (Figure 2a) indicate that the optical band gap and thereby the semiconductor properties of GSCN are maintained with gradually enhanced absorption over the whole range of visible light with increasing amounts of GS included. According to the elemental analysis results (Figure S2), the C/N molar ratios gradually increase with increasing amount of GS, from 0.682 for GSCN-2.5 to 0.691 for GSCN-50. Analysis of thermogravimetric (TG-DTG) curves (Figure S3) has shown that the residual mass of GSCN samples, as expected, depends on the amount of GS added to the solution of cyanamide. The measurements suggest that up to 5 wt % of GS is incorporated into the melon-based carbon nitride structures.

The SEM and TEM images of GSCN (e.g., Figures 2c and S4 for GSCN-20) clearly show the lamellar structure of the nanocomposite. The X-ray patterns (Figure 2b) and electron diffraction patterns (Figure S4) recorded for GSCN do not differ significantly from those of the pure $g\text{-C}_3\text{N}_4$, indicating that the

Table 1. Study of Reaction Conditions^a

entry	catalyst	conv (%) ^b	OH (%) ^c	C=O (%) ^c
1	$g\text{-C}_3\text{N}_4$	0	—	—
2	GS (20 mg)	0	—	—
3	$g\text{-C}_3\text{N}_4$ +GS	0	—	—
4	GSCN-2.5	2	16	84
5 ^d	GSCN-12.5	11	—	67
6	GSCN-20	12	6	94
7	GSCN-50	3	13	87
8 ^e	GSCN-20 (Ar)	0	—	—
9 ^f	GSCN-20 (third)	13	7	93
10 ^f	GSCN-20 (fourth)	12	7	93
11 ^f	GSCN-20 (fifth)	15	8	92
12 ^f	GSCN-20 (sixth)	14	2	98
13 ^g	GSCN-20	0	—	—

^a Typical conditions: 10 mL of CH_3CN , 10 mmol of cyclohexane, 50 mg of catalyst, O_2 (10 bar, note that this pressure might lead to explosion and therefore the catalytic reaction should be conducted in a high-pressure reactor with an explosion-proof pressure sensor), 150 °C, 4 h. ^b Conversions were determined by GC-MS by using anisole as an internal standard. ^c Selectivities of cyclohexanol (OH) and cyclohexanone (C=O). ^d Caprolactone (23%) was detected. ^e Reference experiments in the absence of O_2 . ^f The GSCN-20 catalyst (50 mg) was reused for 3–6 cycles. The catalyst was recycled via centrifugation, washed with CH_3CN , and dried under vacuum oven overnight. ^g 10 mol % of BHT was added.

introduction of GS does not disturb the layered structure of polymeric $g\text{-C}_3\text{N}_4$. This can be further proved by the infrared (FT-IR) spectrum of GSCN (Figure S5), which exhibits typical C–N heterocycle stretches of the extended network connection in the 1100–1600 cm^{-1} region. The surface areas of the modified $g\text{-C}_3\text{N}_4$ also remained nearly the same, even when 50 mg of GS was introduced (see Figure S6). The typical XRD peak of aggregated GS, which appears in the XRD pattern of the mechanical mixture of $g\text{-C}_3\text{N}_4$ and Gr (aggregates of highly reduced GO, bar in Figure 2b), is not observed in the XRD patterns of GSCN. All these observations further reveal that monolayer GSs rather than stacks of homogeneous GSs are distributed in the layered $g\text{-C}_3\text{N}_4$ host, and it is believed that the intensely dispersed state is relevant for the electron exchange between the components.

Our initial studies focused on the oxidation of cyclohexane (CHA), a typical molecule that contains only secondary C–H bonds. CHA is typically oxidized by oxygen gas in the presence of cobalt naphthenate, offering only 4% conversion with 80% selectivity for cyclohexanol (CHON) and cyclohexanone (CHOL).^{1c} The oxidation product CHON is the key raw material in the synthesis of many useful chemical intermediates, such as caprolactone for nylon 6 and adipic acid for nylon 66.^{1c,d} From Table 1, we can see that bare $g\text{-C}_3\text{N}_4$ or GS or the physical mixture of them ($g\text{-C}_3\text{N}_4$ +GS) gave no conversion of CHA. Surprisingly, GSCN- x could favorably activate the molecular oxygen for the oxidation of CHA under the same conditions, the catalytic activity of which can be optimized by adjusting the weight ratio of GS and $g\text{-C}_3\text{N}_4$ components. Low conversion

Table 2. Selective Oxidation of Alkanes^a

Entry	Substrate	Main Product [Selectivity/ %]	Con. [%]
1		4 38	61
2		>99	12
3		3 97	33
4 ^[b]		55 20	76
5 ^[c]		52 12 27	56
6		-	0
7		-	0
8		decan-2-one decan-3-one decan-4-one	trace

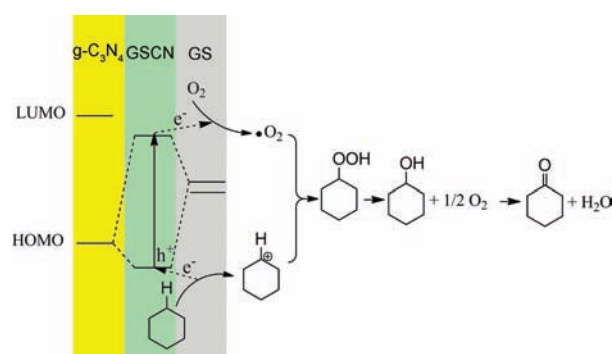
^a Typical conditions: 10 mL of CH₃CN, 10 mmol of substrate, 50 mg of GSCN-20, O₂ 10 bar, 150 °C, 4 h. ^b Temperature = 130 °C. ^c 0.1 g of adamantane was used.

(2–3%) was achieved by GSCN-2.5 and GSCN-50 samples with too little or too much GS. GSCN-12.5 provided a conversion (11%) of CHA with a moderated selectivity (67%) to CHONE. Notably, GSCN-20 gave a good conversion (12%) and a high selectivity (94%) toward CHONE. No overoxidation byproducts, such as adipic acid or valeric acid, were detected in the GC-MS analysis for all the reactions, demonstrating that the selective C–H oxidation is provided from the HOMO of the catalytic dyad of GS layers and g-C₃N₄ layers in a synergistic fashion.

To test the reusability of GSCN in the catalytic reaction, the used GSCN catalyst was recovered from the reaction solution via centrifugation or filtration. The GSCN-20, for instance, was reused for more than six cycles without any obvious loss of its catalytic activity in the catalytic oxidation of CHA (entries 5–8, Table 1); the conversion of CHA was 14% in the sixth cycle with 98% selectivity to CHONE. Since GSCN-20 was the best catalyst for activation of O₂, it was used in subsequent experiments.

In a further set of experiments, we examined the efficacy of transformation of C–H to C=O under the same reaction conditions for a series of substrates, which contain primary, secondary, or tertiary C–H bonds, or two of them. GSCN-20 could promote the oxidation of various secondary C–H bonds (entries 1–4, Table 2) with moderate to high conversions and excellent selectivities toward the corresponding ketones. Tertiary C–H bonds can also be oxidized to corresponding alcohols (entry 5, Table 2). In principle, the conversions of these substrates could be further improved by optimizing the catalytic conditions, recycling of the reactants, or introducing cocatalysts, as currently only standard conditions for evaluating the catalytic performance of GSCN-20 were used. Further improvements in both conversions and critical reaction conditions (e.g.,

Scheme 1. Schematic Representation of the Oxidation Mechanism



high pressure of O₂) are currently underway before these materials can be commercially applied.

All these results indicate that GSCN-20 is an effective but mild catalyst for hydrocarbon oxidation. Under the standard conditions, GSCN-20 gave no conversion of *n*-hexane and DMSO. Hexane has the same secondary CH₂ groups, but this molecule adsorbed much more weakly on the surface of GSCN. This proves that preadsorption of the substrate is a key step. These results revealed that GSCN-20 exhibits moderate to high chemoselectivity for secondary C–H bonds (e.g., entries 2, 3, and 8, Table 2), while substrate selectivity can be adjusted by adsorption equilibria and, therefore, should be useful in overcoming the challenges confronted by metal-mediated catalysis.

As shown in entry 13 of Table 1, GSCN-20 does not catalyze oxidation of CHA in the presence of butylated hydroxytoluene (BHT), a terminating agent that suppresses autoxidation (a free radical chain process). This result strongly suggests that the reaction in our catalytic system progresses via superoxide radical anion ([•]O₂[−]), as summarized in Scheme 1. Our previous results also show that the excited electrons from the conduction band (LUMO) of the C₃N₄ could reduce molecular oxygen to form [•]O₂[−], which stays surface-bound to the C₃N₄ to compensate the positive charge of the hole.^{4d} At the same time, the substrates are oxidized by the HOMO (positive hole) of C₃N₄ and then react with the surface-bound [•]O₂[−], ensuring the selectivity of the catalytic reaction. As a semimetal with a band gap of about zero, graphene has conduction and valence bands that meet at the Dirac point,⁸ so a direct catalytic influence of GSs can be excluded.^{8d} A catalytic influence of the valence bond between GS and C₃N₄ can also be excluded from the solid-state ¹³C NMR analysis (Figure S7) of GSCN. The introduction of GS, however, could obviously shift the HOMO of C₃N₄ to lower energies via, e.g., π–π* or charge-transfer interactions, which can be confirmed by the significant decrease in photoluminescence intensity (Figure S8) as compared with that of g-C₃N₄. Those interactions can be controlled by varying the weight ratio of the components.⁶ We assume that this is why the weight ratio of GS and g-C₃N₄ layers is important for the catalytic activity and selectivity of the hybrid. The as-formed cyclohexyl hydroperoxide could either be directly decomposed or further initiate the autoxidation of CHA (see Supporting Information) to CHOL and CHONE in the presence of GSCN dyads. As expected, the physical mixture, with weak interactions between g-C₃N₄ and GS, offers low catalytic activity.

In summary, we have prepared a series of polymeric carbon nitride composites, GSCN-*x*, using monolayer GS as a nanofiller.

The catalytic reactions presented above clearly indicate that GSCN-20 is a high-performance catalyst to activate molecular oxygen for selective oxidation of secondary C–H bonds of saturated alkanes with good conversion and high selectivity to the corresponding ketones. The synergistic effect of GS and carbon nitride on facilitating these transformations has been unambiguously elucidated. Ease of mass production with high stability, and good activity and selectivity by using molecule oxygen without the assistance of any sacrificial cocatalyst are merits stimulating a wider range of applications for industrially important compounds and intermediates.

■ ASSOCIATED CONTENT

S Supporting Information. Experimental details, more characterization results, and detailed discussions. This material is available free of charge via the Internet at <http://pubs.acs.org>.

■ AUTHOR INFORMATION

Corresponding Author

Xin-Hao.Li@mpikg.mpg.de

■ ACKNOWLEDGMENT

This work was supported by ENERCHEM project of the Max Planck Society, the AvH foundation, the NSFC (20731003), and the National Basic Research Program (2007CB613303) of China.

■ REFERENCES

- (1) For examples, see: (a) Shilov, A. E.; Shul'pin, G. B. *Chem. Rev.* **1997**, *97*, 2879 and references therein. (b) Labinger, J. A.; Bercaw, J. E. *Nature* **2002**, *417*, 507. (c) Maschmeyer, T.; Oldroyd, R. D.; Sankar, G.; Thomas, J. M.; Shannon, I. J.; Kleptko, J.; Masters, A. F.; Catlow, C. R. *Angew. Chem., Int. Ed.* **1997**, *36*, 1639. (d) Kesavan, V.; Sivanand, P. S.; Chandrasekaran, S.; Koltypin, Y.; Gedanken, A. *Angew. Chem., Int. Ed.* **1999**, *38*, 3521. (e) Chen, M. S.; White, M. C. *Science* **2010**, *327*, 566.
- (2) (a) Guengerich, F. P. *Chem. Res. Toxicol.* **2001**, *14*, 611. (b) Nam, W. *Acc. Chem. Res.* **2007**, *40*, 465 and review articles in the special issue.
- (3) For example, see: (a) Das, S.; Incarvito, C. D.; Crabtree, R. H.; Brudvig, G. W. *Science* **2006**, *312*, 1941. (b) Lee, S. J.; Cho, S.-H.; Mulfort, K. L.; Tiede, D. M.; Hupp, J. T.; Nguyen, S. T. *J. Am. Chem. Soc.* **2008**, *130*, 16828. (c) Meeuwissen, J.; Reek, J. N. H. *Nat. Chem.* **2010**, *2*, 615.
- (4) (a) Goettmann, F.; Fischer, A.; Antonietti, M.; Thomas, A. *Angew. Chem., Int. Ed.* **2006**, *45*, 4467. (b) Goettmann, F.; Thomas, A.; Antonietti, M. *Angew. Chem., Int. Ed.* **2007**, *46*, 2717. (c) Wang, X. C.; Maeda, K.; Thomas, A.; Takanabe, K.; Xin, G.; Carlsson, J. M.; Domen, K.; Antonietti, M. *Nat. Mater.* **2009**, *8*, 76. (d) Su, F. Z.; Mathew, S. C.; Lipner, G.; Fu, X. Z.; Antonietti, M.; Blechert, S.; Wang, X. C. *J. Am. Chem. Soc.* **2010**, *132*, 16299.
- (5) (a) Zhang, J. S.; Chen, X. F.; Takanabe, K.; Maeda, K.; Domen, K.; Epping, J. D.; Fu, X. Z.; Antonietti, M.; Wang, X. C. *Angew. Chem., Int. Ed.* **2010**, *49*, 441. (b) Zhang, Y. J.; Mori, T.; Ye, J. H.; Antonietti, M. *J. Am. Chem. Soc.* **2010**, *132*, 6294. (c) Wang, Y.; Zhang, J. S.; Wang, X. C.; Antonietti, M.; Li, H. R. *Angew. Chem., Int. Ed.* **2010**, *49*, 3356. (d) Liu, G.; Niu, P.; Sun, C. H.; Smith, S. C.; Chen, Z. G.; Lu, G. Q.; Cheng, H.-M. *J. Am. Chem. Soc.* **2010**, *132*, 11642. (e) Wang, Y.; Li, H. R.; Yao, J.; Wang, X. C.; Antonietti, M. *Chem. Sci.* **2011**, *2*, 446.
- (6) (a) Beenken, W. J. D. *Chem. Phys.* **2009**, *357*, 144. (b) Sun, Y.; Li, C.; Xu, Y.; Bai, H.; Yao, Z.; Shi, G. *Chem. Commun.* **2010**, *46*, 4740.

(7) (a) Adam, W.; Saha-Möller, C. R.; Ganeshpure, P. A. *Chem. Rev.* **2001**, *101*, 3499. (b) Recupero, F.; Punta, C. *Chem. Rev.* **2007**, *107*, 3800 and references therein.

(8) (a) Geim, A. K.; Novoselov, K. S. *Nat. Mater.* **2007**, *6*, 183–191. (b) Park, S.; Ruoff, R. S. *Nat. Nanotechnol.* **2009**, *4*, 217–224. (c) Allen, M. J.; Tung, V. C.; Kaner, R. B. *Chem. Rev.* **2010**, *110*, 132–145. (d) Dreyer, D. R.; Jia, H.; Bielawski, C. W. *Angew. Chem., Int. Ed.* **2010**, *49*, 6813.

(9) Li, X. H.; Chen, J. S.; Wang, X. C.; Schuster, M. E.; Schlögl, R.; Antonietti, M., unpublished result.